Computers and Structures 128 (2013) 136–145

Contents lists available at ScienceDirect

Computers and Structures

journal homepage: www.elsevier.com/locate/compstruc

A two-scale micromechanical model for aluminium foam based on results from nanoindentation

Jiří Němeček *, Vlastimil Králík, Jaroslav Vondřejc

Czech Technical University in Prague, Faculty of Civil Engineering, Department of Mechanics, Thákurova 7, 16629 Prague 6, Czech Republic

ARTICLE INFO

Article history:
Received 14 February 2013
Accepted 25 July 2013
Available online 13 September 2013

Keywords:
Aluminium foam
Multi-scale model
Nanoindentation
Statistical deconvolution
Elastic properties
Image analysis

ABSTRACT

The main aim of this paper is to develop and verify simple but effective model for elastic properties of a porous aluminium foam system and to compare results received from experimental micromechanics with solutions given by analytical or more advanced numerical methods. The material is characterized by a closed pore system with very thin but microscopically inhomogeneous pore walls (~0.1 mm) and large air pores (~2.9 mm). Therefore, two material levels can be distinguished. The lower level of the proposed model contains inhomogeneous solid matter of the foam cell walls produced from an aluminium melted with admixtures. Elastic parameters as well as volume fractions of microstructural material phases at this level are assessed with nanoindentation and effective properties computed via analytical and numerical homogenization schemes. The effective Young's modulus of the cell walls was found close to 70 GPa irrespective to the used homogenization procedure.

The higher model scale contains homogenized cell walls and a significant volume fraction of air voids (91.4%). Since analytical schemes fail to predict effective properties of this highly porous structure, numerical homogenization based on a simple two dimensional finite element model is utilized. The model geometry is based on foam optical images from which an equivalent beam structure is produced using Voronoi tessellation. Effective foam Young's modulus was found to be 1.36–1.38 GPa which is in relation with ~1.45 GPa obtained from uniaxial compression experiments.

1. Introduction

Metal foams and especially lightweight aluminium foams belong to the group of up-to-date engineering materials with high potential to many applications. Metal foam is a highly porous hierarchical material with a cellular microstructure. Macroscopically, it can be characterized by attractive mechanical and physical properties such as high stiffness and strength in conjunction with very low weight, excellent impact energy absorption, high damping capacity and good sound absorption capability. The usual source material for the production of metal foams are aluminium and aluminium alloys because of low specific density (~2700 kg/m^3), low melting point (~660 °C), non-flammability, possibility of recycling and excellent corrosion resistance. The metal foams are used in applications ranging from automotive and aerospace industries (e.g. bumpers, car body sills, motorcycle helmets) to building industry (e.g. sound proofing panels). Our aim has been to characterize and to model a commercially available foam Alporas produced by Shinko Wire Company, Ltd. This paper, that is devoted to the micromechanical characterization of this material, is an updated and revised version of the conference paper [1].

Alporas [2,3] is characterized with a hierarchical system of pores containing different cell morphologies (in shape and size) depending on the foam density and inhomogeneous material properties of the cell walls [2,4]. A typical cross section of the foam can be seen in Fig. 1 where large pores (having typically 1–13 mm in diameter) are shown with detailed view on thin walls (~100 μm thick).

It follows from its hierarchical microstructure that the mechanical properties of metal foams are governed by two major factors:

(i) cell morphology (shape, size, and distribution of cells) and
(ii) material properties of the cell walls [4].

Traditionally, mechanical properties of metal foams are obtained using conventional macroscopic testing techniques on large samples that can give overall (effective) properties, e.g. [5–10]. However, conventional measurements face significant obstacles in the form of very small dimensions of cell walls, low local bearing capacity, local yielding, and bending of the cell walls. These problems can be overcome using micromechanical experimental methods in which the load–displacement curve is obtained in the

* Corresponding author. Tel.: +420 224354309.
E-mail address: jiri.nemecek@fsv.cvut.cz (J. Němeček).

0045-7949/$ - see front matter © 2013 Elsevier Ltd. All rights reserved.
http://dx.doi.org/10.1016/j.compstruc.2013.07.007

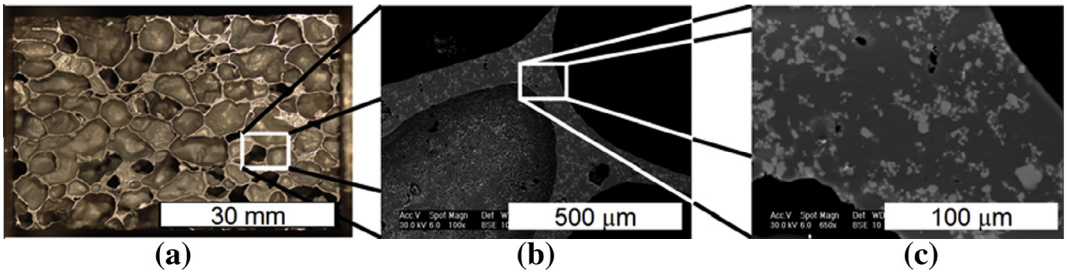

Fig. 1. (a) Overall view on a foam structure (further denoted as Level II); (b) SEM image of a cell wall; (c) detailed SEM image of a cell wall (denoted as Level I) showing Al-rich (dark grey) and Ca/Ti-rich areas (light zones).

sub-micrometer range. A few attempts have been carried out in the past, e.g. [4,7].

The paper develops a bottom-up approach for modeling the elastic properties of metal foam starting from lower level at which microscopic measurements, nanoindentation, and statistical deconvolution for the phase separation [11–13] are utilized. Compared to traditional macroscopic techniques, nanoindentation can distinguish between individual inhomogeneous microstructural entities. The effective cell wall properties have been obtained through analytical and numerical up-scaling techniques [14].

Finally, simple 2-D finite element model for the upper composite scale has been proposed and results validated against full-scale experiments.

2. Experimental part

2.1. Materials and sample preparation

Commercial aluminium foam Alporas® (Shinko Wire Company, Ltd) was used in this study. The manufacturing process of the Alporas is a batch casting process [3] in which 1.5 wt.% of calcium is added to the aluminium molten at 680 °C. Calcium serves as a thickening agent which increases viscosity and stabilizes the air bubbles. The alloy is poured into a casting mold and stirred with an admixture of 1.6 wt.% TiH_2 that is used as a blowing agent. Then, the foamed molten material is cooled down. A typical resulting internal structure of the aluminium foam is shown in Fig. 1(a).

Firstly, a large panel of Alporas (160 × 100 × 60 mm) was polished and scanned with a high resolution scanner. Acquired images were segmented to binary ones and further used in an image analysis. Then, a smaller Alporas block was cut into thin slices (~5 mm) and embedded into epoxy resin to fill the pores. The surface was mechanically grinded and polished to reach minimum surface roughness suitable for nanoindentation. Very low roughness $R_q \approx 10$ nm [15] was achieved on the cell walls. Then, the sample was investigated with electron microscopy and nanoindentation.

2.2. SEM and microstructural analysis

The microstructure of the cell walls was firstly studied in scanning electron microscope (SEM). It was found that a significant inhomogeneity of the microstrutural material phases exists on the level of tens of micrometers (Fig. 1(b) and (c)). Two distinct phases, that exhibit different color in back-scattered electron (BSE) images, can be distinguished. The chemical composition of the two phases was checked with EDX element analysis in SEM. It was found that the majority of the volume (dark zone in Figs. 1(c) and 2(a)) consists of aluminium (~67 wt.%), oxygen (~32 wt.%), and further trace elements (Mg, Ti, Fe, Co, Ni, Cu, Si < 2 wt.%). Lighter zones in Fig. 2 consist of Al (~60 wt.%), O (~30 wt.%), Ca (~5 wt.%), Ti (~5 wt.%) and other elements (<1 wt.%). As expected, the majority of the volume (dark zone) is composed of aluminium and aluminium oxide Al_2O_3 (further denoted as Al-rich area). Lighter zones contain significant amount of calcium and titanium (further denoted as Ca/Ti-rich area). The non-uniform distribution of these zones shows inhomogeneous mixing of the admixtures that are added during the production process.

2.3. Image analysis and porosity

In order to estimate the volume fractions of Al-rich and Ca/Ti-rich areas, image analysis based on previously taken SEM images was employed. Ten arbitrarily chosen areas on wall cross sections were explored. Images were segmented to two phases using a common threshold value of a grey level for all images (Fig. 2). The Ca/Ti-rich area was estimated to cover 22 ± 4% of the whole area.

The overall porosity of the sample was assessed by weighing of a large Alporas panel (knowing the sample dimensions and solid mass density 2700 kg m^{-3}). The porosity reached 91.4% which corresponds to e.g. [3,16]. In other words, solid mass (i.e. the cell walls) occupied only 8.6% of the total volume in the specimen.

Further, the distributions of the cell wall thicknesses and the distribution of pore sizes were studied by means of pore contour detection in the Matlab environment. At first, the contours were generated for every pore in the image and section properties (centroid, area, second moment of inertia) were computed (Fig. 3). The wall thicknesses were calculated as the minimum distance between the neighboring contours. The distribution of the thicknesses is shown in Fig. 4 where a significant peak occurs around ~60 µm which can be understood as a characteristic cell wall thickness.

Then, equivalent ellipses were constructed from contours under the condition that they have the same area and the same principal second moment of inertia. Such assumption led to the evaluation of two main half axes (a_i and b_i) for each equivalent ellipse. In order to characterize the shape of pores, an equivalent ellipse shape factor was defined as the ratio $e_i = \frac{a_i}{b_i}$. The distribution of the shape factor is depicted in Fig. 5. It can be concluded that pores have typically a round shape with the shape factor lying mostly between 1 and 2. The peak with the highest occurrence in Fig. 5 appears around $e_i = 1.15$.

Due to the round shape of pores, it also makes sense to compute an equivalent pore diameter using a circular pore replacement. The distribution of equivalent circular pores is depicted in Fig. 6. Wide distribution of pores with diameters 0–6 mm was found. The mean equivalent diameter was found to be 2.9 ± 1.5 mm for the specific specimen.

2.4. Nanoindentation

Micromechanical properties of the cell walls were measured by means of nanoindentation. The tests were performed using the